# VIBRATORY LOADS REDUCTION ANALYSIS OF ACTIVE TRAILING-EDGE FLAP BLADES UTILIZING PIEZOELECTRIC BUCKLING ACTUATORS

Jae-Sang Park
Research Professor
Dept. of Aerospace Information Engineering
Konkuk University
Seoul, KOREA
smartrotor@gmail.com

Sung-Nam Jung
Professor
Dept. of Aerospace Information Engineering
Konkuk University
Seoul, KOREA
snjung@konkuk.ac.kr

Yung-Hoon Yu
Professor
Dept. of Aerospace Information Engineering
Konkuk University
Seoul, KOREA
yhoon@konkuk.ac.kr

## Abstract

This paper shows the vibratory loads reduction analysis of Active Trailing-edge Flap (ATF) blade utilizing piezoelectric buckling actuators. The present ATF blade is based on the properties and configuration of previous NASA/Army/MIT Active Twist Rotor (ATR) blade, but it has the trailing-edge flap with 20% blade span length and 15% blade chord length. The trailing-edge flap for the present ATF blade is actuated by piezoelectric buckling actuators. Up to now, various piezoelectric stack actuators have been developed for the ATF blade, but they can produce only relatively small displacement, thus they should require the amplification mechanism which results in the weight increase and the complexity. However, since the piezoelectric buckling actuator used in this work can produce the large rotation from the buckling of the beam due to the free elongation of piezoelectric stack actuator, it does not need the complex amplification mechanism. Using the simple mathematical model, the piezoelectric buckling actuator is designed and its actuation performance is investigated. Following the modeling of the piezoelectric buckling actuator, a multi-body dynamics modeling for the ATF blade utilizing piezoelectric buckling actuators is conducted. In this modeling, various multi-body element libraries such as rigid body, rigid/elastic joints and elastic beam are used to construct the ATF rotor system modeling in the forward flight condition. Through the simulation, the result shows that the ATF blade utilizing the piezoelectric buckling actuators may reduce vibratory loads at the hub of the rotor significantly although much lower input-voltage is applied to the actuator.

## Introduction

Vibratory loads in rotorcrafts results from a variety of sources such as the main rotor system, the aerodynamic interaction between the rotor and the fuselage, the tail rotor, the engine and transmission, and atmospheric turbulence, which generally has low frequencies. However, the most significant source of rotorcraft vibration is the main rotor because of the unsteady aerodynamic environment acting on highly flexible rotating blades in forward flight condition, as shown in Figure 1.

In order to relieve such problems, during the last two decades, active control methodologies to modify directly the periodic aerodynamic loads acting upon the rotor blades have been examined. These may be broadly classified as Higher Harmonic Control (HHC, [1]) and Individual Blade Control (IBC, [2]).

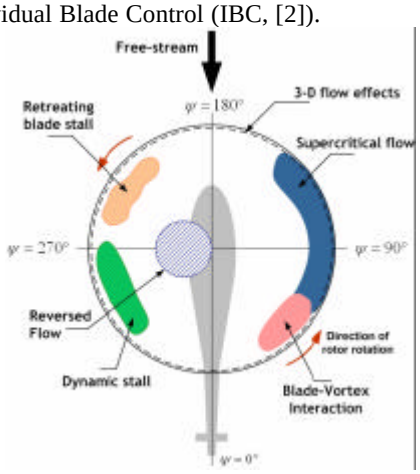


Figure 1 Aerodynamic environment of helicopters in forward flight condition

HHC was introduced in the 1970s and has been shown to reduce vibration and noise by implementing active control of the rotor swashplate to change the pitch at the root of the blades. IBC typically uses hydraulically-actuated pitch links to achieve active control of each blade independently.

Although both HHC and IBC showed several outstanding results for both either small or full-scaled model [1-3] and flight test [4], some difficulties arise in providing the necessary hydraulic power in the rotating system. This constraint results from adverse power requirement and limitation on excitation frequency in case of HHC, and extreme mechanical complexity of hydraulic sliprings in case of IBC.

Recently, by introducing smart materials, especially piezoelectric materials, various active rotor control methods using piezoelectric actuators, such as Active Trailing-edge Flaps (ATF, Figure 2(a)) or Active Twist Rotor (ATR, Figure 2(b)), have been suggested.

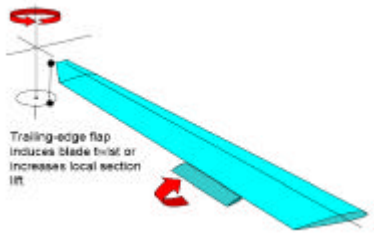


(a) Active Trailing-edge Flap (ATF) blades

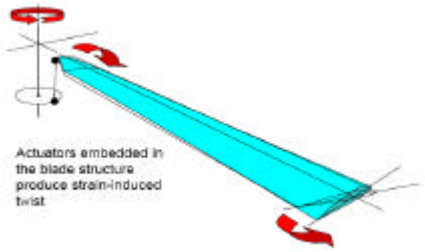


(b) Active Twist Rotor (ATR) blades

Figure 2 Active rotor controls using piezoelectric actuators

The numerical and experimental researches on the ATF rotor blade have been extensively. The ATF blade uses a small flap on each blade to generate the desired unsteady aerodynamic loads. This scheme can be effective, but uses less power than the conventional IBC techniques. In ATF technique, a partial span trailing-edge flap is located at the outboard region of the blade. A number of numerical researches [5-8], some wind tunnel tests [9], full-scale whirl tower test [10, 11] and full-scale BK-117 test [12] of the active flap have been demonstrated. Their results showed the potential of the ATF blade to significantly reduce the vibratory loads, alleviate noise, and enhance the rotor performance and handling qualities.

With researches on the ATF blades, over the past decade, various piezoelectric actuators in order to deflect a trailing-edge flap of a rotor blade have been developed. Piezoelectric bender actuators (Figure 3) were developed for the small-scaled wind-tunnel models [13-15]. Piezoelectric benders consists of two or more piezoelectric sheets stacked together such that actuating the layers on opposite side of the neutral axis results in an opposite strain which may cause the entire bender to be deflected. After improvements in the actuator design, approximately ±4° flap deflections were obtained at a rotor speed of 1800 RPM [14]. Closed loop wind tunnel tests showed a dramatic vibration reduction in 4/rev fixed frame loads.

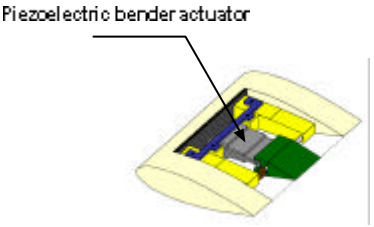


Figure 3 Schematic diagram of a trailing-edge flap using piezoelectric bender actuators

As another type of piezoelectric actuator, there are piezoelectric stack actuators constructed by laminating multiple piezoelectric layers (Figure 4). The piezostack actuators can be used in both small- and full-scaled models and have a larger force output than the bender actuators. However, they can only produce a relatively small displacement, and that should be amplified in order to achieve a required flap deflection. This limitation needs more complex amplification mechanisms such as a double lever mechanism [16] or X-frame mechanism [17].

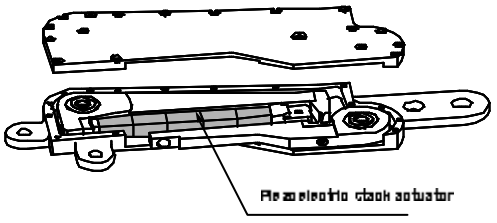


Figure 4 Double Lever (L-L) actuator using piezoelectric stack

These amplification mechanisms result in the weight increase of the blade and complexity. Thus, to solve this problem, recently the piezoelectric buckling actuator was developed [18]. As shown in Figure 5, the piezoelectric stack actuator produces the free elongation strain, which causes the buckling of the beam. As a result, the large rotation of the output shaft is obtained. This concept can be used to deflect the trailing-edge flap of the rotor blade without any complex amplification mechanism Thus, the piezoelectric buckling actuator is very simple, compact and lightweight.

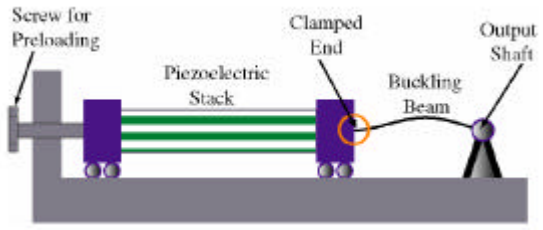


Figure 5 Concept of piezoelectric buckling actuator

In this work, the simple mathematical modeling for the piezoelectric buckling actuator to deflect the trailing-edge flap both upward and downward is conducted. The buckling beam actuator is modeled base on the Euler-Bernoulli beam theory with eccentric compressive loads. The relationship between the input-voltage to the piezoelectric stack actuator and the flap deflection angle is predicted.

Following the modeling of the piezoelectric buckling actuator, the multi-body dynamics modeling for the ATF blade utilizing the piezoelectric buckling actuator is performed. In the modeling, various multi-body elements such as rigid body, rigid/elastic joints and elastic beams are used. The properties and configuration of the present ATF blade are based on the NASA/Army/MIT ATR blade [19]. However, the present ATF blade has the trailing-edge flap with 20% blade span length and 15% blade chord length. By using IBC mode, for the forward flight condition simulation, the most effective actuation frequency and control phase angle are obtained to reduce the vibratory loads at the hub of the rotor system. The numerical result shows that the ATF blade using the piezoelectric buckling actuator may reduce the vibratory loads of the helicopter significantly although much lower input-voltage to the actuator is applied.

## Mathematical Modeling of Piezoelectric Buckling Actuators

Based on the concept of the piezoelectric buckling actuator [18], the piezoelectric buckling actuator for the ATF blade is designed as in Figure 6. Two piezoelectric stack actuators are used in order to deflect the trailing-edge flap both upward and downward. To determine the deflection direction of the flap, each piezoelectric stack actuator has the geometric eccentric offset with respect to the beam. Therefore, if the lower piezoelectric stack actuator is used, the trailing-edge flap is deflected downward, while when the upper piezoelectric stack actuator is activated, the trailing-edge flap is deflected upward. Thus, the sequential actuation of lower and upper piezoelectric stack actuators deflects the flap from downward to upward.

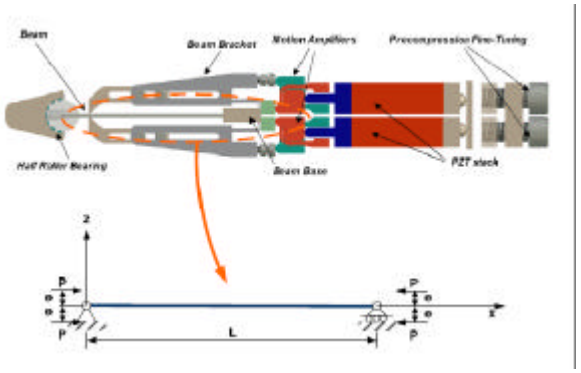


Figure 6 Piezoelectric buckling actuator for trailing-edge flap

In this paper, the buckling actuator is modeled based on the simply supported Euller-Bernoulli beam under eccentric compressive loads as shown in Figure 6. The eccentric compressive loads $P$ is generated from the free elongation of piezoelectric stacks. The compressive loads $P$ is given as

$$P = nd_{33}V_{pp}E_p\frac{A}{h} \tag{1}$$

where $n$ is the number of piezoceramic layers of the stack, $d_{33}$ is the piezoelectric strain constant and $V_{pp}$ is the peak-to-peak input-voltage. In addition, $E_p$ is the Young's modulus, $A$ is the cross-section area and $h$ is the height of piezoelectric stack actuator.

When the compressive loads $P$ with eccentric offset $e$ are applied to the beam, the equilibrium equation of the beam is expressed as

$$w_{,xxxx} + k^2 w_{,xx} = 0 \tag{2}$$

where $w$ is the transverse deflection and $k$ is $P/EI$.

The boundary conditions are given by

$$\begin{aligned} w(0) &= 0 \\ w(L) &= 0 \\ EIw_{,xx}(0) &= Pe \\ EIw_{,xx}(L) &= Pe \end{aligned} \tag{3}$$

The solution for Equation (2) can be expressed as

$$w(x) = A_1 \sin kx + A_2 \cos kx + A_3 x + A_4 \tag{4}$$

When the boundary conditions, Equation (3), is applied to Equation (4), finally the solution can be given as

$$w(x) = e\left[1 - \cos kx - \tan\frac{kL}{2}\sin kx\right] \tag{5}$$

From the derivative of Equation (5) with respect to $x$, the shaft rotation angle can be predicted.

### Multi-Body Modeling of ATF Blade

In this section, the multi-body dynamic modeling techniques for the ATF blade in forward flight condition are discussed. For the multi-body modeling of the ATF blade, DYMORE [20] is used in this work. DYMORE is a nonlinear flexible multi-body dynamics analysis which has various multi-body element libraries, such as rigid bodies, mechanical joints, and elastic beams. Deformable bodies are modeled with the finite element method. The equations of equilibrium are formulated in a Cartesian inertial frame. Constraints are modeled using the Lagrange multiplier technique. The formulation of beams is based on the geometrically exact beam theory considering the arbitrarily large displacements, finite rotations and small strains [21], but uses the displacement-based form instead of the mixed form. To analyze aerodynamic loads, DYMORE uses finite-state dynamic inflow aerodynamics model [22]. This model is constructed by applying the acceleration potential theory to the rotor aerodynamics problem with a skewed cylindrical wake. More specifically, the induced flow at the rotor disk was expanded in terms of modal functions. As a result, a three-dimensional, unsteady induced-flow aerodynamics model with finite number of states is derived in time domain. This model is an intermediate level of wake representation between the simplest momentum and the most complicate free wake methodologies.

The hub is modeled as a rigid body, and connected with a revolute joint underneath. It is under a prescribed rotation with nominal rotating speed $\Omega$. Root retention is a passive elastic beam rigidly attached to the hub, and the reaction loads at the attachment point are extracted and added over four of them to give the hub vibratory loads. Because the ATF rotor system is fully articulated, three revolute joints are consecutively located between the root retention and the active flap blade to represent flap, lead-lag, and feathering hinges.

In this modeling, the flapping and lead-lag hinges are coincident. The ATF blade can be divided into 3 regions: passive inner blade (blade segment 1), active flap blade (blade segment 2) and passive outer blade (blade segment 3) regions. Each blade region is discretized during the analysis at least three beam elements per blade, each with the 3rd-order interpolation polynomials. Finally, to represent trailing-edge flap in DYMORE, as shown in Figure 7, several rigid joints and elastic beams for the brackets and flap are introduced. The flap is assumed to be 20% of the blade span and 15% of the chord, located at 75% of the blade radius.

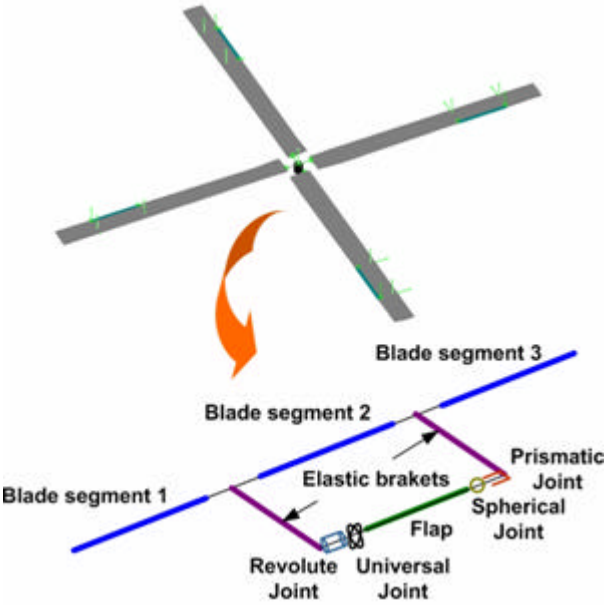


Figure 7 Multi-body modeling for the ATF blade

The flap deflection is described as a prescribed rotation considering IBC mode as

$$\begin{aligned} d(t) = {} & d_{\text{amplitude}} \times \\ & \cos\left\{2p w_{\text{actuation}}\left(t - f_{\text{controlphase}}\right) + 2N_{\text{act}} p f_{\text{blade}\,i}\right\} \end{aligned} \tag{6}$$

### Flap Deflection Performance

The piezoelectric buckling actuator should be included in the blade inside structure. The present ATF blade uses a NACA 0012 airfoil cross-section with chord length of 0.1077m and the flap chord length is assumed to be 15% of the main blade chord length. Figure 8 represents the piezoelectric buckling actuator inside the cross-section of the ATF rotor. The piezoelectric buckling actuator is located at the second cell of the cross-section. In this study, two PZT-5A stack actuators with 144 piezoelectric layers and an Aluminum buckling beam are used.

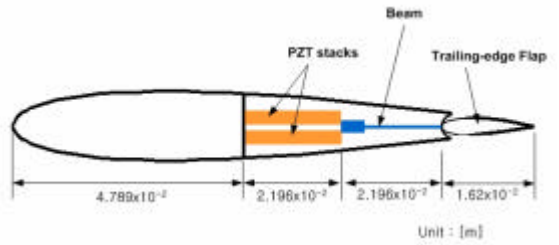


Figure 8 Piezoelectric buckling actuator inside the ATF blade cross-section

Figure 9 shows the relationship between the input-voltage and the trailing-edge flap deflection angle. As you can see, when the target deflection angle is 4 deg., the input-voltage of about 5.1 Volt is required. This value of input-voltage to meet the target flap deflection is much lower as compared with that of the previous piezoelectric actuators used for the other researches for the ATF blades.

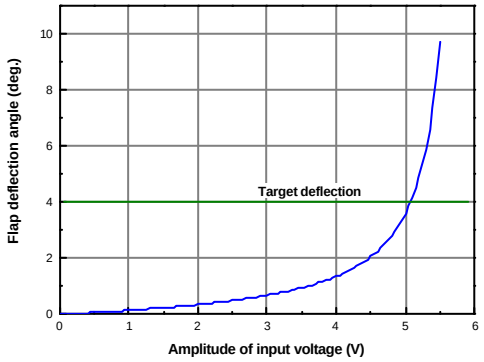


Figure 9 Flap deflection angle performance of piezoelectric buckling actuator

### Vibratory Loads Reduction Analysis of the ATF Blade

This section describes the vibratory loads reduction analysis of the ATF blade using the piezoelectric buckling actuator. The present ATF blade has similar properties and the same external configuration of the previous NASA/Army/MIT ATR blade. Table 1 shows the properties of the NASA/Army/MIT ATR blade [19].

Table 1 Properties of the NASA/Army/MIT ATR blade

| | |
|---|---|
| Rotor type | Fully articulated |
| Number of blades, b | 4 |
| Blade chord, c | 0.108 m |
| Blade radius, R | 1.397 m |
| Solidity, bc/pR | 0.0982 |
| Lock number | 9.0 |
| Airfoil shape | NACA 0012 |
| Blade linear pretwist | -10 deg. |
| Hinge offset | 7.62 cm |
| Root cutout | 31.75 cm |
| Pitch axis | 25% c |
| Elastic axis | 19.6% c |
| Center of gravity | 23.2% c |
| Nominal rotor speed | 687.5 RPM |
| Mass per unit span, m | 0.710 kg/m |
| 1st torsional frequency at nominal rotor speed | 6.97/rev |

By using constructed DYMORE modeling for the ATF blade, specifically, hub reaction loads of the rotor system are estimated. These vibratory loads are obtained from summation of all the loads in the four root retention elements. Figure 10 illustrates the simulated vertical component of the hub shear forces developed in the ATF system. For this example, the amplitude of input-voltage is 5.1V. In addition, the steady-state trim condition is that advance ratio $m = 0.140$ , rotor-shaft angle of attack $a_s = -1°$, and thrust coefficient $C_T = 0.0066$.

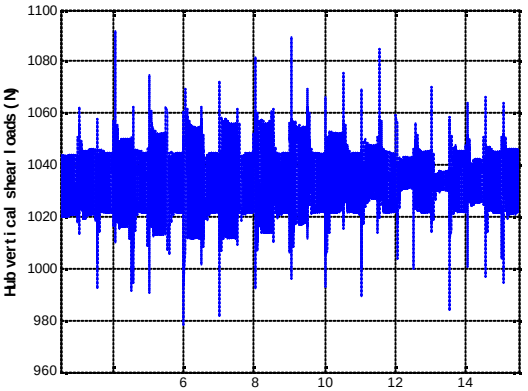


Figure 10 Simulated time history of the hub vertical shear loads with 3/rev actuation

The time domain analysis result can be transferred to frequency domain to investigate the magnitude of the frequency content of interest, which is 4/rev in the present four-bladed rotor system. Figure 11 shows 4/rev hub shear vibratory loads with 3, 4 and 5/rev actuation during the same steady-state trim condition.

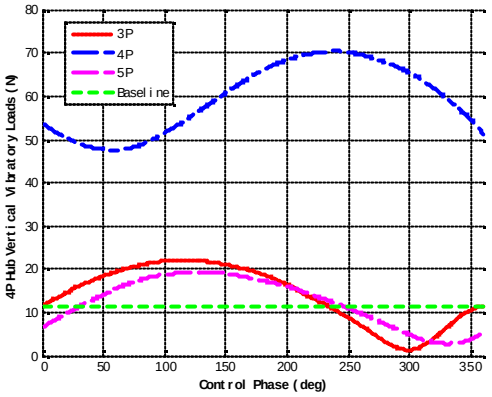


(a) Vertical component

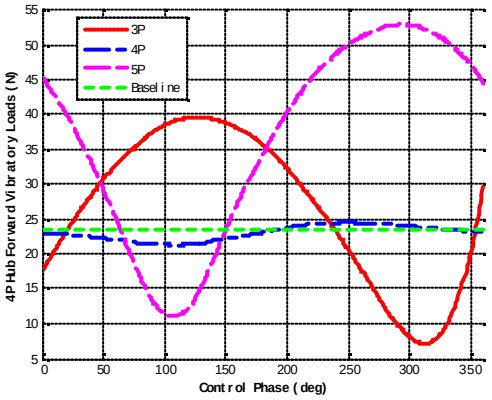


(b) Forward component

Figure 11 Variation of 4/rev hub shear vibratory loads with 3, 4 and 5/rev with respect to control phase

As one can see, 3/rev actuation appears to be the most effective in reducing the hub shear vibratory loads in both cases of vertical and forward components. Particularly, as compared with the baseline value, 3/rev actuation with 303°control phase gives approximately 89% reduction of the hub vertical shear loads.

It should be noted that these vibratory loads reduction can be obtained when only 5.1V input-voltage is imposed to each piezoelectric buckling actuator. To achieve this level of the vibratory loads reduction, if the previous ATF blade using previous amplification mechanism is considered, 100~200V input-voltage to PZT stack actuator is required in general. Furthermore, as compared with the ATR controls, the ATR blade using Active Fiber Composites (AFC) requires 1,000 V twist actuations. Since the piezoelectric buckling actuator can produce the large rotation angle with much lower input-voltage and without any complex amplification mechanism, the ATF blade utilizing the piezoelectric buckling actuator is capable of reducing the vibratory loads of rotorcrafts more efficiently.

## Conclusions

This paper investigates the vibratory loads reduction of the ATF blade using the piezoelectric buckling actuator. The piezoelectric buckling actuator can give the large rotation of the trailing-edge flap without any amplification mechanism since the free elongation of the piezoelectric stack actuator causes the buckling of the beam connected to the trailing-edge flap. By the simple mathematical modeling, the flap deflection performance is investigated. Although much lower-input voltage is applied to the piezoelectric stack actuator, the piezoelectric buckling actuator can meet the target deflection angle. Furthermore, a multi-body dynamics modeling for the ATF blade for the forward flight analysis is conducted. In the modeling various multi-body elements such as rigid body, rigid/elastic joints and elastic beams are used. The prescribed displacement considering IBC mode is considered to describe the flap deflection. The numerical simulation shows that the ATF blade with the piezoelectric buckling actuator may reduce 4/rev hub vibratory loads of 4 bladed rotor system significantly and more efficiently.

## Acknowledgements

This work was supported by Brain Korea 21 in 2008. The authors would like to express their acknowledgment to Dr. O. A. Bauchau from the Georgia Institute of Technology for providing access to the analysis code DYMORE.

## References

[1] Shaw, J., Albion N., Hanker E. J., and Teal, R. S., "Higher Harmonic Control: Wind Tunnel Demonstration of Fully Effective Vibratory Hub Force Suppression," Journal of the American Helicopter Society, Vol. 31, (1), 1989, pp. 14-25.

[2] Ham, N. D., "Helicopter Individual-Blade-Control Research at MIT 1977-1985," Vertica, Vol. 11, (1/2), 1987, pp. 109-122.

[3] Nguyen, K., Betzina, M., and Kitaplioglu, C.,

"Full-Scale Demonstration of Higher-Harmonic Control for Noise and Vibration Reduction on the XV-15 Rotor," American Helicopter Society 56th Annual Forum, Virginia Beach, VA, May 2000.

[4] Wood, E. R., Power, R. W., Cline, J. H., and Hammond, C. E., "On Developing and Flight Testing a Higher Harmonic Control System," Journal of the American Helicopter Society, Vol. 30, (1), 1985, pp. 3-20.

[5] Millott, T. A., and Friedmann, P. P., "Vibration Reduction in Helicopter Rotors Using an Active Control Surface Located on the Blade," 33rd AIAA/ASME/ASCE/AHS/ ASC Structures, Structural Dynamics and Materials Conference, Dallas TX, April 1992.

[6] Milgram, J. H., and Chopra, I., "Helicopter Vibration Reduction with Trailing-Edge Flaps," 36th AIAA/ASME/ASCE/AHS/ASC Structures, Structural Dynamics and Materials Conference, New Orleans LA, April 1995.

[7] Straub, F. K., and Hanson, A. A., "Aeromechanic Considerations in the Design of a Rotor with Smart Material Actuated Trailing Edge Flaps," American Helicopter Society 52nd Annual Forum, Washington DC, June 1996.

[8] Fulton, M. V., and Ormiston, R., "Small-Scale Rotor Experiments with On-Blade Elevons to Reduce Blade Vibratory Loads in Forward Flight," American Helicopter Society 54th Annual Forum, Washington DC, May 1998.

[9] Dawson, S., Hassan, A., Straub, F. K., and Tadghighi, H., "Wind Tunnel Test of an Active Flap rotor: BVI Noise and Vibration Reduction," American Helicopter Society 51st Annual Forum, Fort Worth TX, May 1995.

[10] Straub, F. K., Kennedy, D. K., Stemple, A. D., Anand, V. R., Birchette, T. S., "Development and Whirl Tower Test of the SMART Active Flap Rotor," SPIE: Smart Structures and Integrated Systems, San Diego CA, March 2004.

[11] Enenkl, B., Kloppel, V., and Preibler, D., "Full Scale Rotor with Piezoelectric Actuatred Blade Flaps," 28th European Rotorcraft Forum, Bristol, United Kingdom, 2002.

[12] Dieterich, O., Enenkl, B., and Roth, D., "Trailing Edge Flaps for Active Rotor Control Aeroelastic Characteristics of the ADASYS Rotor System," American Helicopter Society 62nd Annual Forum, Pheonix AZ, May 2006.

[13] Samak, D. K., Chopra, I., "Design of High Force, High Displacement Actuators for Helicopter Rotors," Smart Structures and Intelligent Systems; Proceedings of the

[14] Koratkar, N. A., Chopra, I, "Wind Tunnel Testing of a Smart Rotor Model with Trailing-Edge Flaps," Journal of the American Helicopter Society, Vol. 47, (4), 2002, pp. 263-272.

[15] Hall, S. R., Spangler, R., "Piezoelectric Actuators for Helicopter Rotor Control," 31st AIAA/ASME/ASCE/AHS/ASC Structures, Structural Dynamics and Materials Conference, Long Beach, CA, April 1990.

[16] Lee, T.-O., and Chopra, I., "Design Issues of a High-Stroke, On-Blade Piezostack Actuator for a Helicopter Rotor with Trailing-Edge Flaps," Journal of Intelligent Material Systems and Structures, Vol. 11, 2000, pp. 328-342.

[17] Prechtl, E. F., and Hall, S. R., "X-Frame Actuator Servo-Flap Actuation System for Rotor Control," SPIE: Smart Structures and Integrated Systems, San Diego CA, March 1998.

[18] Jiang, J., and Mockensturm, E. M., "A Novel Motion Amplifier Using Axial Driven Buckling Beam," 2003 ASME International Mechanical Engineering Congress, Washington DC, November 2003.

[19] Wilbur, M. L., Mirick, P. H., Yeager, Jr. W. T., Langston, C. W., Cesnik, C. E. S., and Shin, S.-J., "Vibratory Loads Reduction Testing of the NASA/Army/MIT Active Twist Rotor," Journal of the American Helicopter Society, Vol. 47, (2), 2002, pp. 123-133.

[20] Bauchau, O. A., "Computational Schemes for Flexible, Nonlinear Multi-Body Systems," Multibody System Dynamics, Vol. 2, 1998, pp. 169-225.

[21] Hodges, D. H., "A mixed variational formulation based on exact intrinsic equations for dynamics of moving beams," International Journal of Solids and Structures, 26(11):1253-73, 1990.

[22] Peters, D. A. and He, C. J., "Finite State Induced Flow Models Part II: Three-Dimensional Rotor Disk," Journal of Aircraft, 32(2): 323-333, 1995.